DALTON
FULL PAPER

The synthesis of $C[Si(CH_3)_2X]_3SiX_3$ compounds (X = H, Cl, Br and OH) and the molecular structure of $C[Si(CH_3)_2H]_3SiH_3$ in the gas phase; a study by electron diffraction and *ab initio* molecular orbital calculations †

Carole A. Morrison,[a] David W. H. Rankin,*[a] Heather E. Robertson,[a] Paul D. Lickiss[b] and Phindile C. Masangane[b] ‡

[a] *Department of Chemistry, University of Edinburgh, West Mains Road, Edinburgh, UK EH9 3JJ*
[b] *Chemistry Department, Imperial College of Science, Technology and Medicine, London, UK SW7 2AY*

Received 13th April 1999, Accepted 3rd June 1999

A series of new hexafunctional tetrasilylmethane derivatives, $C[Si(CH_3)_2X]_3SiX_3$, have been prepared. In addition a comprehensive structural study of the parent compound $C[Si(CH_3)_2H]_3SiH_3$ has been undertaken. A full search of the potential energy surface has been performed *ab initio*. Results indicate the presence of a total of eleven distinct conformational minima with a total energy range of only 3 kJ mol^{-1}, with evidence for appreciable energy barriers to internal rotation. The analysis of gas-phase electron diffraction data has been undertaken for this eleven-conformer model and a satisfactory fit has been obtained.

Introduction

There has been considerable interest in recent years in the chemistry and structures of tetrasilylmethane derivatives as the steric hindrance at silicon centres in such compounds can lead to unusual reactivity and novel structural features.[1,2] The majority of tetrasilylmethanes contain only one or two silicons with substituents other than methyl groups at which reactions can be relatively easily carried out. For example, compounds of the type $C[Si(CH_3)_3]_3SiRR'X$ and $C[Si(CH_3)_3]_2(SiRR'X)[Si(CH_3)_2Y]$ (where R and R′ = alkyl or aryl; X and Y = H, halide, or pseudohalide) have been of particular interest from a mechanistic point of view.[3] Several studies have led to an interest in compounds in which all four of the silicons bear reactive substituents, for example $C(SiH_3)_4$ has been proposed as a precursor to silicon-containing thin films *via* chemical vapour deposition[4] and $C[Si(CH_3)_2H]_4$ has been used as a potential free-radical reducing agent.[5]

The work presented in this paper consists of two parts. First, as part of our continuing interest in polyfunctional tetrasilylmethanes the synthesis of a range of compounds $C[Si(CH_3)_2X]_3SiX_3$ (where X = H, Cl, Br, and OH) is now reported. Secondly, extensive *ab initio* calculations over the full potential energy surface for the simple hexahydridosilane $C[Si(CH_3)_2H]_3SiH_3$ have been performed, in addition to the determination of its gas-phase structure by electron diffraction.

Results and discussion

Synthesis and characterisation

The synthetic route to $C[Si(CH_3)_2X]_3SiX_3$ species is outlined in Fig. 1. The cleavage of Si–CH_3 bonds by iodine monochloride has been used previously in the preparation of $C[Si(CH_3)_2Cl]_4$ from $C[Si(CH_3)_3]_4$,[6] and the reaction between $C[Si(CH_3)_3]_3SiCl_3$ and ICl proceeds cleanly to give the hexachloride $C[Si(CH_3)_2Cl]_3SiCl_3$ as an air-stable, white crystalline solid. A similar reaction of $C[Si(CH_3)_3]_3SiCl_3$ with IBr was found to be much slower. ^{1}H NMR spectroscopy showed that although a stepwise reaction to give $C[Si(CH_3)_2Br][Si(CH_3)_3]_2SiCl_3$, $C[Si(CH_3)_2Br]_2[Si(CH_3)_2]SiCl_3$ and $C[Si(CH_3)_2Br]_3SiCl_3$ appeared to be occurring, the reaction was incomplete after eight weeks. None of the mixed halogen-containing compounds was isolated.

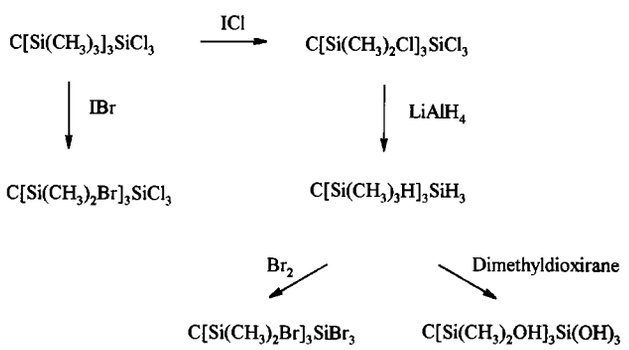

Fig. 1 Synthetic routes to new $C[Si(CH_3)_2X]_3SiX_3$ compounds.

Clean reduction of the hexachloride proved difficult to achieve. The common method for the reduction of chlorosilanes containing the bulky $C[Si(CH_3)_3]_3$ group,[7] (*i.e.* reduction using $LiAlH_4$ in THF) led to a mixture of the required hexahydrido compound together with the trisilylmethane $C[Si(CH_3)_2H]_3H$ [which has also been prepared from the reaction between $CHBr_3$, Mg and $Si(CH_3)_2ClH$][8] by cleavage of the central C–SiX_3 bond and other unidentified compounds. Similar C–Si bond cleavage is seen in the reaction of $C[Si(CH_3)_2Ph]_3SiCl_3$ with $LiAlH_4$, which affords $C[Si(CH_3)_2Ph]_3H$,[9] and the formation of $C[(SiH_3)_3]^-$ in the reduction of $C(SiBrH_2)_4$ by $LiAlH_4$.[4] This presumably reflects the stabilising effect of silyl groups α to a carbanion and hence the good leaving group ability of trisilylmethyl ions. Variation of the reaction time and the amount

† *Supplementary data available*: GED data analysis model and coordinates for 11 conformers of $C[Si(CH_3)_2H]_3SiH_3$; Brookhaven (.pdb) files of 11 conformers. For direct electronic access see http://www.rsc.org/suppdata/dt/1999/2293/.

‡ Present address: Chemistry Department, University of Swaziland, P/Bag 4, Kwaluseni, Swaziland, Southern Africa.

of $LiAlH_4$ used did not allow a clean product to be formed but the use of a $LiAlH_4$/toluene two-phase system containing benzyltriethylammonium chloride as a phase transfer catalyst,[10] a method which has successfully been used in the synthesis of $C(SiH_3)_4$ from $C(SiBrH_2)_4$,[4] did allow $C[Si(CH_3)_2H]_3SiH_3$ to be prepared in good yield as a highly volatile solid. The IR spectrum of $C[Si(CH_3)_2H]_3SiH_3$ shows two strong bands in the Si–H stretching region at 2110 cm^{-1} and 2140 cm^{-1}, which were assigned to the tertiary Si–H and primary Si–H stretches respectively by comparison with frequencies of 2090 cm^{-1} and 2138 cm^{-1} observed for $C[Si(CH_3)_2H]_3H$[8] and $C[Si(CH_3)_3]_3SiH_3$,[11] respectively. The ^{29}Si NMR data for $C[Si(CH_3)_2H]_3SiH_3$ are also in good agreement with those of $C[Si(CH_3)_2H]_3H$ and $C[Si(CH_3)_3]_3SiH_3$. The SiH_3 signal is a quartet at δ −61.3 with $^1J_{Si-H}$ = 200 Hz while that of $C[Si(CH_3)_3]_3SiH_3$ is also centred at δ −61.3 with a coupling constant of 198 Hz. The $Si(CH_3)_2H$ signal of $C[Si(CH_3)_2H]_3SiH_3$ is a doublet at δ −13.8 with $^1J_{Si-H}$ = 188 Hz, comparing well with δ −15.5 and a coupling constant of 185 Hz found in the $Si(CH_3)_2H$ signal of $C[Si(CH_3)_2H]_3H$.[8] The proton coupled ^{29}Si NMR spectrum of $C[Si(CH_3)_2H]_3SiH_3$ revealed further couplings, the SiH_3 group split into a quartet ($^3J_{Si-H}$ = 3.5 Hz) by the three equivalent $Si(CH_3)_2\mathit{H}$ hydrogens, and the $\mathit{Si}(CH_3)_2H$ signal, split by the three equivalent SiH_3 hydrogens ($^3J_{Si-H}$ = 3.5 Hz) (as well as by the coupling to the CH_3 groups).

The bromination of $C[Si(CH_3)_2H]_3SiH_3$ with a 1.0 M solution of Br_2 in CCl_4 was found to be rapid and gave the expected hexabromide $C[Si(CH_3)_2Br]_3SiBr_3$ in near quantitative yield. The use of a deficiency of Br_2 allowed the intermediate bromides to be identified by ^1H NMR spectroscopy, which showed that initial bromination occurred at the $Si(CH_3)_2H$ groups, and that $C[Si(CH_3)_2Br]_3SiH_3$ formed as a significant intermediate in the reaction. Unfortunately, the partially brominated compounds could not be isolated individually.

The faster bromination of the more sterically hindered tertiary hydrides, $Si(CH_3)_3H$, than the primary hydrides, SiH_3, is consistent with the results of El-Durini and Jackson who found the rates of bromination of $Si(C_2H_5)_3H$, $Si(CH_3)_3H$ and $Si(C_6H_5)H_3$ to be 13.4, 1.10 and 0.65 mol^{-1} s^{-1} respectively.[12] In such reactions it was concluded that steric effects are relatively unimportant, but that it is the presence of electron-releasing groups, increasing positive charge build-up at silicon during the reaction that increases the rate. The novel highly brominated silane $C[Si(CH_3)_2Br]_3SiBr_3$ was isolated as colourless crystals. As in the case of $C[Si(CH_3)_3]_3SiBr_3$, it is air stable, a very unusual property for a bromosilane, which would normally be expected to undergo rapid hydrolysis with atmospheric moisture to give HBr, together with silanols and siloxanes. Although air stable, the hexabromide is hydrolysed in aqueous acetone solution to give a mixture of unidentified siloxanes, and the partially brominated species, which are less bulky, react readily with atmospheric moisture, also to give unidentified siloxanes.

At room temperature the ^1H NMR signal (270 MHz) of $C[Si(CH_3)_2Br]_3SiBr_3$ was found to be a broad resonance between δ 1.1 and 1.2. This suggested that a dynamic process was occurring and that hindered rotation around the central Si–C bonds at this temperature was relatively slow. The temperature dependence of the ^1H NMR spectrum was then studied between 70 °C and −70 °C on a 270 MHz spectrometer and at 70 °C the spectrum, as expected, showed a sharp singlet at δ 1.22 which began to split unsymmetrically into two main peaks as the temperature of the sample was lowered. Expansion of the signal recorded at −70 °C showed the presence of two main resonances in an approximate 1:1 ratio, together with about six smaller ones. This is consistent with the presence of one predominant conformer in which the methyl groups within a single $Si(CH_3)_2Br$ group are inequivalent but the three $Si(CH_3)_2Br$ groups overall are equivalent. The presence of several smaller resonances is consistent with the presence of at least one less symmetrical conformer. The freezing out of more than one conformer in tetrasilylmethanes at low temperature has also been observed for the related compounds $C[Si(CH_3)_2I]_4$ and $C[Si(CH_3)_2Br]_4$,[13] and other tetrasilylmethane derivatives have been shown to exhibit hindered rotation at temperatures readily accessible by NMR spectroscopy.[14,15] Using the Eyring equation[16] with values of 298 ± 5 °C for the coalescence temperature and 40 Hz for the separation between the two main peaks at low temperature, an activation energy of 63.5 ± 1 kJ mol^{-1} for methyl group exchange was calculated. Similar studies for $C[Si(CH_3)_3]_3SiBr_3$ have shown two methyl group exchange processes to occur between room temperature and −70 °C with free energies of activation calculated to be 45 ± 0.5 and 52.2 ± 0.5 kJ mol^{-1}.[15] The related trichlorosilane $C[Si(CH_3)_2Ph]_3SiCl_3$ also shows hindered rotation within a conformer at low temperature, also having two distinct methyl group resonances whose exchange has a free energy of activation of 53.1 kJ mol^{-1} at −10 °C.[15] Interestingly, the ^{29}Si NMR spectra of $C[Si(CH_3)_2Br]_3SiBr_3$ showed no resonances when recorded at room temperature at 53.6 MHz and at 99.6 MHz but at 50 °C signals were as expected: a singlet at δ 18.66 which was assigned to $\mathit{Si}(CH_3)_2Br$ and another singlet at δ −36.59 assigned to $\mathit{Si}Br_3$. Again this can be attributed to hindered rotation about the Si–C bonds at room temperature.

X-Ray diffraction studies on the only crystals of $C[Si(CH_3)_2Br]_3SiBr_3$ that could be obtained show a twofold disorder of the Si_4 tetrahedron generating a "cube" of eight half Si atoms with a carbon atom at the centre. The six bromine atoms are disordered over twelve sites (effectively bridging the edges of the cube) and obscuring the positions of the methyl groups which must alternate with them in the crystal. This model is consistent with the presence of many isomers co-crystallising or with a single isomer in eight different orientations randomly distributed through the crystal and superimposed to give the observed image.[17]

Although $C[Si(CH_3)_2H]_3SiH_3$ is a potentially useful precursor to dendritic organosilanes it would also be useful to have precursors containing Si–O functions, particularly silanols, that could be used as cores for dendrimers. Silanes are readily oxidised by dioxiranes to give the corresponding silanols and this provides a mild, high-yield, and effective route for the synthesis of sensitive, polyfunctional silanols.[18] The new silane, $C[Si(CH_3)_2H]_3SiH_3$, when treated with six equivalents of dimethyldioxirane solution gave the new silanol $C[Si(CH_3)_2OH]_3Si(OH)_3$ in excellent yield. Unfortunately, the silanol tends to undergo condensation reactions in acetone, pentane or chlorinated solvents, but it is stable in the solid state as a fine white powder. Its ^{29}Si NMR spectrum shows two signals; one at δ −43.5 assigned to the $\mathit{Si}(OH)_3$ resonance compares well with δ −39.9 and −40.1 of the $\mathit{Si}(OH)_3$ group in $C[Si(CH_3)_3]_3Si(OH)_3$ and $C[Si(CH_3)_2Ph]_3Si(OH)_3$, respectively,[9] and one at δ 10.5 assigned to the $\mathit{Si}(CH_3)_2(OH)$ resonance is comparable to the δ 13.4 assigned for the $\mathit{Si}(CH_3)_2(OH)$ resonance in $C[Si(CH_3)_3]_3Si(CH_3)_2OH$.[19] Silanols are known to crystallise to give a variety of hydrogen bonded structures[18] and it was thought of interest to see if the structure of $C[Si(CH_3)_2OH]_3Si(OH)_3$ might combine the unusual hydrogen-bonded features of the triol $C[Si(CH_3)_3]_3Si(OH)_3$, which crystallises to give discrete three-dimensional hexameric hydrogen bonded cages,[20] and $C[Si(CH_3)_2OH]_4$ which forms an infinite three-dimensional network.[21] Unfortunately all attempts at obtaining crystals suitable for X-ray crystallography have so far proved unsuccessful and are impeded by the silanol's ease of condensation.

Ab initio calculations for $C[Si(CH_3)_2H]_3SiH_3$

A full search of the potential energy surface located eleven different local minima for $[(CH_3)_2SiH]_3CSiH_3$, a surprisingly large number for a molecule comprising only 35 atoms. Moreover, the minima were found to lie at points on the potential energy

Table 1 Partial geometries of the eleven conformers of $C[Si(CH_3)_2H]_3SiH_3$ calculated *ab initio* at 6-31G*/MP2 (r_e/Å, </°). Branch types 'a', 'b' and 'c' denotes branch torsional angles Si(2)–C(1)–Si–H of *ca.* 160°, 40° and −80°, respectively

	'aaa'	'bbb'	'ccc'	'aab'	'aca'	'abb'	'cbb'	'cca'	'ccb'	'acb'	'abc'
Bond distances											
*r*C(1)–Si(2)	1.877	1.891	1.884	1.881	1.879	1.885	1.888	1.882	1.886	1.884	1.884
*r*C(1)–Si(3)	1.900	1.900	1.897	1.899	1.902	1.897	1.896	1.902	1.900	1.901	1.893
*r*C(1)–Si(13)	—	—	—	1.898	1.895	1.896	1.892	1.897	1.893	1.897	1.902
*r*C(1)–Si(23)	—	—	—	1.900	1.900	1.900	1.901	1.896	1.896	1.896	1.900
*r*Si(2)–H(33)	1.490	1.489	1.489	1.489	1.490	1.488	1.488	1.490	1.489	1.489	1.488
*r*Si(2)–H(34)	—	—	—	1.490	1.490	1.490	1.489	1.489	1.489	1.490	1.489
*r*Si(2)–H(35)	—	—	—	1.490	1.489	1.490	1.489	1.490	1.489	1.490	1.491
*r*Si(3)–H(4)	1.496	1.497	1.498	1.496	1.495	1.497	1.496	1.495	1.496	1.496	1.498
*r*Si(3)–C(5)	1.888	1.888	1.888	1.888	1.888	1.889	1.889	1.888	1.888	1.888	1.890
*r*Si(3)–C(6)	1.889	1.889	1.888	1.889	1.887	1.889	1.889	1.886	1.888	1.887	1.889
*r*Si(13)–H(14)	—	—	—	1.496	1.496	1.497	1.497	1.497	1.497	1.495	1.496
*r*Si(13)–C(15)	—	—	—	1.887	1.889	1.888	1.889	1.889	1.888	1.889	1.887
*r*Si(13)–C(16)	—	—	—	1.889	1.890	1.887	1.889	1.888	1.889	1.888	1.888
*r*Si(23)–H(24)	—	—	—	1.496	1.496	1.497	1.497	1.496	1.497	1.497	1.497
*r*Si(23)–C(25)	—	—	—	1.888	1.887	1.890	1.888	1.890	1.887	1.889	1.889
*r*Si(23)–C(26)	—	—	—	1.888	1.888	1.888	1.888	1.887	1.889	1.889	1.889
Bond angles											
<Si(2)–C(1)–Si(3)	110.2	106.7	107.8	108.4	109.3	108.8	107.9	107.5	106.8	107.9	109.9
<Si(2)–C(1)–Si(13)	—	—	—	110.4	109.4	108.0	107.8	109.1	109.1	109.0	106.2
<Si(2)–C(1)–Si(23)	—	—	—	108.8	109.3	106.9	105.1	108.9	106.0	107.7	107.9
<C(1)–Si(3)–H(4)	107.6	107.4	107.8	108.3	107.7	108.2	107.1	107.9	107.4	108.2	108.3
<C(1)–Si(3)–C(5)	114.1	112.4	112.3	112.8	111.8	112.7	113.2	112.3	112.4	112.9	113.5
<C(1)–Si(3)–C(6)	112.3	114.0	113.5	112.7	114.1	113.1	113.7	113.2	113.5	112.1	112.8
<H(4)–Si(3)–C(5)	107.7	107.2	108.1	108.5	107.9	108.7	107.5	107.8	108.2	108.4	108.3
<H(4)–Si(3)–C(6)	108.8	107.4	107.9	108.4	107.5	108.0	107.7	107.4	108.1	108.0	108.3
<C(5)–Si(3)–C(6)	106.2	108.0	107.2	106.1	107.5	105.9	107.4	108.0	107.0	107.1	105.4
<C(1)–Si(13)–H(14)	—	—	—	107.8	108.2	107.4	107.3	107.6	107.5	107.6	106.7
<C(1)–Si(13)–C(15)	—	—	—	114.2	112.4	113.5	113.9	112.8	113.0	113.1	113.9
<C(1)–Si(13)–C(16)	—	—	—	112.4	113.6	113.4	113.0	113.4	113.6	113.1	113.5
<H(14)–Si(13)–C(15)	—	—	—	107.5	108.5	108.3	107.8	107.3	107.4	107.1	108.1
<H(14)–Si(13)–C(16)	—	—	—	107.9	108.2	107.2	106.9	107.4	107.3	107.1	107.4
<C(15)–Si(13)–C(16)	—	—	—	106.8	105.7	106.7	107.6	108.1	107.8	108.4	106.9
<C(1)–Si(23)–H(24)	—	—	—	107.7	107.3	107.2	106.8	108.3	106.8	107.1	107.0
<C(1)–Si(23)–C(25)	—	—	—	112.6	112.6	113.8	114.0	113.4	113.9	113.3	113.5
<C(1)–Si(23)–C(26)	—	—	—	113.2	113.1	112.7	112.6	111.8	113.1	113.7	113.1
<H(24)–Si(23)–C(25)	—	—	—	108.9	107.2	107.9	107.4	108.1	107.6	106.9	107.7
<H(24)–Si(23)–C(26)	—	—	—	107.1	106.9	107.1	107.2	108.2	106.9	108.0	107.2
<C(25)–Si(23)–C(26)	—	—	—	107.1	109.4	107.9	108.5	106.7	108.3	107.9	107.9
Torsional angles											
τSi(2)–C(1)–Si(3)–H(4)	158.8	43.8	−80.1	163.4	158.1	163.2	−77.9	−76.4	−78.2	165.0	161.3
τSi(2)–C(1)–Si(13)–H(14)	—	—	—	154.9	−76.9	43.0	43.2	−80.0	−79.8	−77.2	39.8
τSi(2)–C(1)–Si(23)–H(24)	—	—	—	45.2	161.4	44.8	40.9	164.4	40.3	−43.3	−77.4

Table 2 Absolute energies (calculated *ab initio*) and relative abundance of all conformers modelled in the electron diffraction analysis

Conformer[a]	Multiplicity	Energy/E_h 6-31G*/MP2	Zero-point energy (ZPE) correction 6-31G*/HF	Absolute energy (ZPE corrected)	Population in gas phase[b]
'aaa'	1	−1436.050072	0.303010	−1435.747062	0.03
'bbb'	1	−1436.049974	0.302480	−1435.747494	0.04
'ccc'	1	−1436.050837	0.302932	−1435.747905	0.05
'aab'	3	−1436.050232	0.302740	−1435.747492	0.11
'aca'	3	−1436.050361	0.302696	−1435.747665	0.13
'abb'	3	−1436.049731	0.302597	−1435.747134	0.08
'cbb'	3	−1436.049891	0.302703	−1435.747188	0.09
'cca'	3	−1436.050462	0.302598	−1435.747864	0.16
'ccb'	3	−1436.050241	0.302832	−1435.747409	0.11
'acb'	3	−1436.050298	0.302553	−1435.747745	0.14
'abc'	3	−1436.049575	0.302781	−1435.746794	0.06

[a] See text and Fig. 2 for structural definitions. [b] Calculated on the basis of a Boltzmann distribution, relative to the lowest energy conformer 'ccc' at 373 K. Abundances are then corrected for the effects of multiplicity and normalised.

surface within a range of only *ca.* 3 kJ mol^{-1}, predicting that all eleven conformers will exist in the gas phase, and thus be of comparable importance in the GED refinement. Partial geometries obtained from the 6-31G*/MP2 optimisations only are presented in Table 1. [A full set of Brookhaven (pdb) files are available as Electronic Supplementary Information.] The abso-

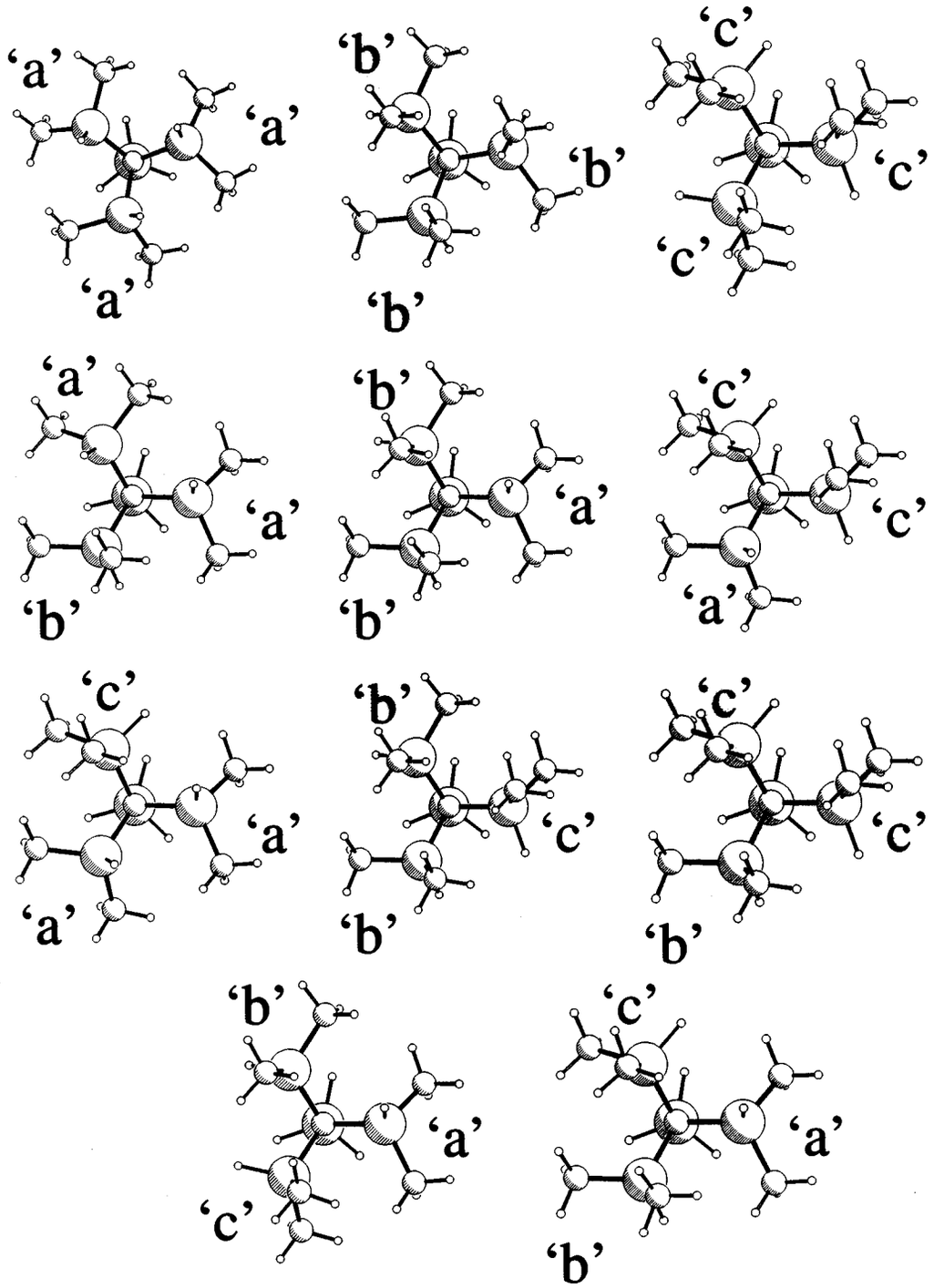

Fig. 2 Molecular structures of the eleven conformers of $C[Si(CH_3)_2H]_3SiH_3$. Torsional angles Si(2)C(1)SiH denoted 'a' *ca.* 160°, 'b' *ca.* 40° and 'c' *ca.* −80°.

lute energies obtained in the 6–31G*/MP2 set of calculations, with zero-point energy corrections obtained from the 6-31G*/HF frequency calculations, are listed in Table 2.

This system, comprising three branches with three different possible orientations for each branch, will have a total of 27 (3^3) different possible conformations, some of which are equivalent. With reference to Fig. 2 and 3 (for atom labelling) and Table 1 it is clear that the geometries calculated fall into tightly defined categories. In compounds of the type $A(XY_3)_4$, 1,3-interactions between atoms or groups Y cause the XY_3 groups to twist away from perfectly staggered conformations, usually by 15–20°. All four groups must twist in the same sense. In this case, therefore, to within a close approximation only three different values of the branch torsional angles [*i.e.* Si(2)–C(1)–Si(3)–H(4), Si(2)–C(1)–Si(13)–H(14) and Si(2)–C(1)–Si(23)–H(24)] were observed, *ca.*160° (labelled type 'a'), 40° (type 'b') and −80° (type 'c'). Thus there are three conformers with C_3 symmetry (and multiplicities of one) labelled 'aaa', 'bbb' and 'ccc', and eight remaining conformers with C_1 symmetry (multiplicities of three) arise from all other possible combinations of the three different branch types (see Fig. 2). Further conformations are possible if the twisting of branch methyl groups relative to the branch hydrogens H(4), H(14) and H(24) is considered. However with all eleven minima found the methyl torsional twists are very slight, with most groups less than 5° away from a perfectly staggered conformation. This structural feature is therefore considered to be negligible, and no further minima have been found.

A rigid scan of the potential energy surface linking two minima (corresponding to conformers 'cca' to 'ccb'; 6-31G*/HF level, see Table 3) was undertaken to determine the height of the potential energy barrier to free rotation between the two con-

Table 3 Results from *ab initio* (6-31G*/HF) scan of potential energy surface between minima corresponding to conformers 'cca' and 'ccb'

	Dihedral angle branch 'a' ⟶ 'b'	Absolute energy/E_h	Δ^a
1	166.6	−1434.78839	0.0
2	156.4	−1434.78662	+4.6
3	146.2	−1434.78031	+21.2
4	136.0	−1434.76989	+48.6
5	125.8	−1434.76098	+80.0
6	115.6	−1434.75875	+77.8
7	105.4	−1434.75860	+78.2
8	95.2	−1434.75594	+85.2
9	85.0	−1434.75632	+84.2
10	74.8	−1434.76463	+62.4
11	64.6	−1434.77495	+35.3
12	54.4	−1434.78197	+16.9
13	44.2	−1434.78487	+9.0

[a] Differences quoted in kJ mol^{-1}, relative to the minimum 'cca'.

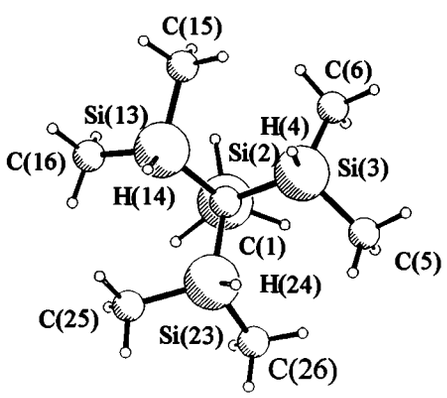

Fig. 3 Atom numbering scheme adopted for $C[Si(CH_3)_2H]_3SiH_3$.

formers. Although a rigid scan can only give an approximation of the barrier height, a value of more than 80 kJ mol^{-1} was calculated, indicating that the minima must relate to two very distinct features on the potential energy surface. Perhaps this is not surprising, as a substantial geometry change of *ca.* 120° is required to any one branch torsional angle to convert between two conformer types. It can therefore be concluded that in all likelihood all geometries calculated will exist as distinct entities; the groups are not simply freely rotating between the eleven minima found.

Gas-phase electron diffraction (GED)

GED model. In light of the unexpected prediction from *ab initio* calculations that eleven independent conformers of near equal energy will exist in the gas phase, several structural assumptions had to be made in order to reduce the number of geometric parameters needed to describe such an exceptionally large system. Full details of the model comprising 45 geometric parameters can be found in the Electronic Supplementary Information. The main structural assumptions made are listed here for ease of reference.

Si(2,3,13,23) branches. The biggest structural assumption made was to describe all branches in all eleven conformers by just three different branch types 'a', 'b' and 'c', as detailed above. This greatly simplified the model required but still made it possible to model all Si–C(1)–Si angles and torsions calculated *ab initio* to within a mean deviation of just 2°. Thus three parameters were required to describe the angles Si(2)–C(1)–Si(3,13 or 23), and just seven torsional angles were required to separate the three branch types to give the conformer arrangements shown in Fig. 2. On the basis of geometries calculated *ab initio* the conformers were assumed to possess only three different Si–C distances: silyl *r*Si(2)–C(1), middle *r*Si(3,13 or 23)–C(1) and branch *r*Si–C(methyl). Only two different Si–H distances were modelled [those in the SiH_3 groups and those in the $Si(CH_3)H$ groups]. One parameter was used to describe all 66 C(1)–Si–C branch angles [*e.g.* <C(1)Si(3)C(5 or 6) *etc.*] and one parameter to define all 33 C(1)–Si–H branch angles. Calculated values for both parameters fell over a range of just 2° (see Table 1), justifying the use of one parameter in each case.

Methyl groups. All were considered to be identical and possess local C_{3v} symmetry. In light of the *ab initio* calculations they were also assumed to be perfectly staggered with respect to the branch hydrogens H(4), H(14) and H(24).

SiH_3 group. This group was assumed to be identical in all eleven conformers and to possess local C_{3v} symmetry.

GED refinement. On the basis of the *ab initio* calculations detailed above, eleven different conformers were modelled in the refinement of the GED data collected for $C[Si(CH_3)_2H]_3SiH_3$. The relative weightings of the conformers were fixed at values obtained from a consideration of the Boltzmann distribution of population states, relative to the lowest energy conformer 'ccc' (6-31G*/MP2; ZPE corrected, see Table 3), at the temperature of the GED data collection.§ These relative weightings were then corrected for the effects of multiplicity (*i.e.* the weightings of the C_3 conformers reduced to one third of their initial value) and then normalised. The values used in the final GED refinement are given in the last column of Table 2.

The presence of a large number of similar interatomic distances and of some parameters involving hydrogen (which is a poor scatterer of electrons) of low multiplicity prevented a complete structure determination for $C[Si(CH_3)_2H]_3SiH_3$ using just experimental data, even with the simplifications built into the model. In such cases it is our practice to include information obtained theoretically to allow complete structural determination using the SARACEN method.[22] The essential feature of this method is that information calculated *ab initio* is introduced into the refinement procedure as additional observations (or restraints), the weight of any observation being assigned according to the level of convergence achieved in a series of graded *ab initio* calculations. By employing the SARACEN method in the present work it has been possible to refine the values of all structural parameters and all significant amplitudes of vibration. The final refinement is then the best fit to all available information, both experimental and theoretical, and represents the most probable structure, avoiding subjective preference for one particular type of data. The values of all additional observations used in the refinement can be found in Table 4 together with their respective weightings (uncertainties).

The results from the SARACEN refinement, based on GED data supplemented with *ab initio*-based restraints, are given in Table 4 where they are compared with parameters derived computationally.¶ In general most geometric parameters refined to values in good agreement with those calculated *ab initio*. Most notably the freely refining parameters, which define the key features on the radial distribution curve (see Fig. 4), refined to values within acceptable agreement with calculated geometries. The distance C–H (p_1), which gives an unusually large contribution to the radial distribution curve, refined to 1.089(4) Å, just out within one esd of the average *ab initio* value of 1.094 Å. The average Si–C distance (p_3, peak three in the radial distribution curve) refined to 1.884(1) Å, compared to the average calculated

§ Calculated changes in entropy (6-31G*/HF) for all eleven conformers fell over a range of just 0.02 kJ K^{-1}. The conformation of the gas phase mixture was determined based on ΔH values, not ΔG.

¶ For large, floppy molecules, such as those detailed in this paper, it is not realistic to expect to obtain a reliable r_α structure based on harmonic rectilinear (parallel and perpendicular) vibrational corrections. In particular the perpendicular corrections are very poorly calculated, and introduce errors greater than those they are meant to solve. The structures presented in this paper are therefore of type r_a.

Table 4 Structural parameters obtained by gas-phase electron diffraction and *ab initio* calculations (*r*/Å, </°)

	Parameter[a]	GED (restrained results) (r_a)[b]	*Ab initio* (6-31G*/MP2) (r_e)[c]
	Independent parameters		
p_1	*r*C–H	1.089(4)	av. 1.094
p_2	<Si–C–H (branch)	109.8(5)	range 109.0–113.0
p_3	av. *r*Si–C (silyl + middle + branch)	1.884(1)	1.890
p_4	Δ *r*Si–C [middle − av.(branch + silyl)]	0.013(2)	0.012(2)
p_5	Δ *r*Si–C (branch − silyl)	0.005(2)	0.004(2)
p_6	av. *r*Si–H av. (branch + silyl)	1.502(12)	1.480(20)
p_7	Δ *r*Si–H (branch − silyl)	0.010(5)	0.010(5)
p_8	<C(1)–Si–C (branch)	113.8(4)	av. 113.2
p_9	<C(1)–Si–H (branch)	106.4(9)	107.0(10)
p_{10}	<H–Si–C (branch)	107.1(7)	108.0(10)
p_{11}	Δ <Si(2)–C(1)–Si ('a' + 'b' + 'c')	107.0(6)	108.3(10)
p_{12}	Δ <Si(2)–C(1)–Si ['a' − av.('b' + 'c')]	1.6(4)	1.3(5)
p_{13}	Δ <Si(2)–C(1)–Si ('b' − 'c')	−1.5(5)	−1.2(5)
p_{14}	av. <Si(branch)–C(1)–Si(branch)	109.9(9)	110.6
p_{15}	Δ <Si–C(1)–Si [av.('ab' + 'bb' + 'cb') − av.('aa' + 'ac' + 'bc' + 'cc')]	2.7(4)	2.8(5)
p_{16}	Δ <Si–C(1)–Si [av.('ab' + 'bb') − 'cb']	−2.6(5)	−2.6(5)
p_{17}	Δ <Si–C(1)–Si('ab' − 'bb')	0.7(5)	0.8(5)
p_{18}	Δ <Si–C–(1)–Si[av. ('aa' + 'cc') − av.('ac' + 'bc')]	1.8(5)	1.8(5)
p_{19}	Δ <Si–C(1)–Si['cc' − 'aa']	0.2(5)	0.2(5)
p_{20}	Δ <Si–C(1)–Si['ac' − 'bc']	0.9(5)	0.9(5)
p_{21}	<C(1)–Si(2)–H (centre)	109.0(9)	109.0(10)
p_{22}	twist angle SiH_3	−80.5(18)	−80(2)
p_{23}	'aaa' τC(1)–Si(2)–Si–H	158.7(18)	159(2)
p_{24}	'bbb' τC(1)–Si(2)–Si–H	43.8(18)	44(2)
p_{25}	'ccc' τC(1)–Si(2)–Si–H	−79.8(18)	−80(2)
p_{26}	'aab' τC(1)–Si(2)–Si(3)–H(4)	163.7(18)	163(2)
p_{27}	'aab' τC(1)–Si(2)–Si(3)–H(14)	154.8(18)	155(2)
p_{28}	'aab' τC(1)–Si(2)–Si(3)–H(24)	45.6(18)	45(2)
p_{29}	'aca' τC(1)–Si(2)–Si(3)–H(4)	158.2(18)	158(2)
p_{30}	'aca' τC(1)–Si(2)–Si(13)–H(14)	−76.5(18)	−77(2)
p_{31}	'aca' τC(1)–Si(2)–Si(23)–H(24)	161.2(18)	161(2)
p_{32}	'abb' τC(1)–Si(2)–Si(3)–H(4)	163.4(18)	163(2)
p_{33}	'abb' τC(1)–Si(2)–Si(13)–H(14)	43.2(18)	43(2)
p_{34}	'abb' τC(1)–Si(2)–Si(23)–H(24)	44.8(18)	45(2)
p_{35}	'cbb' τC(1)–Si(2)–Si(3)–H(4)	−78.0(18)	−78(2)
p_{36}	'cbb' τC(1)–Si(2)–Si(13)–H(14)	43.4(18)	43(2)
p_{37}	'cbb' τC(1)–Si(2)–Si(23)–H(24)	40.7(18)	41(2)
p_{38}	'cca' τC(1)–Si(2)–Si(3)–H(4)	−75.8(17)	−76(2)
p_{39}	'cca' τC(1)–Si(2)–Si(13)–H(14)	−79.9(18)	−80(2)
p_{40}	'cca' τC(1)–Si(2)–Si(23)–H(24)	164.4(18)	164(2)
p_{41}	'ccb' τC(1)–Si(2)–Si(3)–H(4)	−78.3(18)	−78(2)
p_{42}	'ccb' τC(1)–Si(2)–Si(13)–H(14)	−79.6(18)	−80(2)
p_{43}	'ccb' τC(1)–Si(2)–Si(23)–H(24)	40.4(17)	40(2)
p_{44}	'abc' τC(1)–Si(2)–Si(3)–H(4)	161.6(18)	161(2)
p_{45}	'abc' τC(1)–Si(2)–Si(13)–H(14)	39.7(18)	40(2)
p_{46}	'abc' τC(1)–Si(2)–Si(23)–H(24)	−77.4(18)	−77(2)
p_{47}	'acb' τC(1)–Si(2)–Si(3)–H(4)	165.3(18)	165(2)
p_{48}	'acb' τC(1)–Si(2)–Si(13)–H(14)	−77.2(18)	−77(2)
p_{49}	'acb' τC(1)–Si(2)–Si(23)–H(24)	43.3(18)	43(2)
	Dependent parameters		
	*r*Si–C (silyl)	1.878(1)	av. 1.883
	*r*Si–C (middle)	1.893(2)	av. 1.898
	*r*Si–C (branch)	1.883(1)	av. 1.888
	*r*Si–H (silyl)	1.497(12)	av. 1.490
	*r*Si–H (branch)	1.508(12)	av. 1.497
	<Si(2)–C(1)–Si ('a')	108.1(6)	av. 109.2
	<Si(2)–C(1)–Si ('b')	105.7(6)	av. 107.0
	<Si(2)–C(1)–Si ('c')	107.2(6)	av. 108.3
	<Si–C(1)–Si ('aa')	109.6(10)	av. 110.2
	<Si–C(1)–Si ('ab')	110.3(10)	av. 111.0
	<Si–C(1)–Si ('ac')	107.4(10)	av. 108.1
	<Si–C(1)–Si ('bb')	111.0(10)	av. 111.7
	<Si–C(1)–Si ('bc')	108.3(10)	av. 109.0
	<Si–C(1)–Si ('cb')	113.2(10)	av. 113.9
	<Si–C(1)–Si ('cc')	109.8(10)	av. 110.4

[a] See text for model description. Note: 'silyl' = *r*Si(2)–C(1), 'middle' = *r*Si(3,13 or 23)–C(1) and 'branch' = *r*Si–C(methyl) distances (see Fig. 3 for atom numbering scheme). Abbreviations used: *r* = bond distance, < = angle, τ = dihedral angle, av. = average, Δ = difference, 'a,b,c' = branch types; see the text and Fig. 2 for details. [b] Estimated standard deviations (e.s.d.s) obtained in the least-squares refinement are given in parentheses, quoted to 1σ. [c] *Ab initio* data quoted with uncertainties are SARACEN restraints used in the GED refinement; *ab initio* values quoted as averages are derived from values calculated for each given parameter over all eleven conformers.

Table 5 Selected distances, common to all level conformer models, from the SARACEN refinement of $C[Si(CH_3)_2H]_3SiH_3$

Position on radial distribution curve	Atom pair	Amplitude, *u*/Å
peak 1	C(5)–H(7)	0.066(5)
peak 2	Si(3)–H(4)	0.086 (fixed)
	Si(2)–H(33)	0.085 (fixed)
peak 3	Si(3)–C(5)	0.039(2)
	Si(2)–C(1)	0.030 {tied to *u*[Si(2)–C(5)]}
	Si(3)–C(1)	0.041 {tied to *u*[Si(2)–C(5)]}
peak 4	$Si(3)\cdots H_{methyl}$	0.09(1)
peak 5	Si···Si	0.118(3)

value of 1.890 Å. The Si–C–H (branch) angle (p_2), which in conjunction with p_1 and p_3 defines the position of the fourth peak on the radial distribution curve (labelled $rH_{methyl}\cdots Si$), refined to 109.8(5)°, which falls within the range of values calculated for this angle (109.0–113.0°). The branch C(1)–Si–C angle (p_8), which along with p_3 directly positions the C···C distances under peak 5, refined to 113.8(4)°, compared to the calculated average value of 113.2°.

The two branch angles, <Si(2)–C(1)–Si and <Si(branch)–C–Si(branch), p_{11} and p_{14}, which together with the Si–C distances define the Si···Si distances under peak 5, were found to be heavily correlated in the refinement (see Table 5). Unrestrained, both parameters may drift to unrealistic values. A restraint was therefore applied to parameter 11 (p_{14} left unrestrained), resulting in both parameters returning values in the least-squares analysis within *ca.* 1° of the calculated values.

The remaining parameters which could not refine to realistic values, because they refer either to subtle geometry differences between correlated bond distances or angles (*i.e.* parameters 4, 5, 7, 12, 13, and 15–20) or to parameters involving hydrogen (parameters 7, 9, 10, 21, 22 and 23–45) were assigned *ab initio* based restraints to aid their refinement. All restrained parameters returned values in the least-squares analysis in agreement with their imposed restraints to within one or two e.s.d.s.

In addition to all 45 geometric parameters, four amplitudes of vibration, corresponding to groups of similar distances under the four most prominent peaks on the radial distribution curve, were also refined. The groups chosen correspond to all C–H distances for the eleven conformers under peak 1, the Si–C distances under peak 3, $rH_{methyl}\cdots Si$ (peak 4) and the Si···Si distances under peak 5. All amplitudes refined to reasonable values, in good agreement with those calculated *ab initio*.

The final R_G factor recorded for this eleven-conformer refinement is 0.075, indicating that the data are of good quality and a good fit between model and experiment has been obtained. The final experimental and difference radial distribution and molecular scattering curves are shown in Fig. 4 and 5, respectively. A selective listing of bonding distances and amplitudes of vibration common to all eleven conformers (due to the structural approximations made as listed above) is given in Table 5. The final correlation matrix obtained is given in Table 6. A full set of coordinates is available in Table 1 of the Electronic Supplementary Information.

Table 6 Correlation matrix (× 100) for the SARACEN refinement of $C[Si(CH_3)_2H]_3SiH_3$. Only elements with absolute values greater than 50 are shown. k_2 is a scale factor; *u* is an amplitude of vibration

	p_{10}	p_{11}	p_{14}	k_2
p_8	−55	65	−69	
p_{11}			−86	
u(C–Si)				72

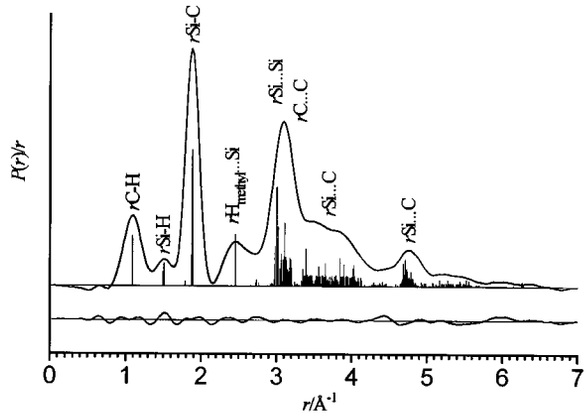

Fig. 4 Experimental and difference (experimental − theoretical) radial distribution curves for the multi-conformer analysis of $C[Si(CH_3)_2H]_3SiH_3$. Before Fourier inversion the data were multiplied by $s.\exp[(-0.002s^2)/(Z_{Si} - f_{Si})(Z_C - f_C)]$.

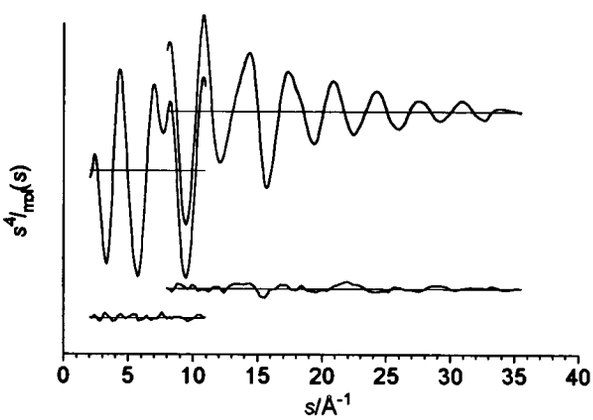

Fig. 5 Experimental and final weighted difference (experimental − theoretical) molecular scattering intensities for the multi-conformer analysis of $C[Si(CH_3)_2H]_3SiH_3$.

Experimental

Synthesis

Preparation of $C[Si(CH_3)_2Cl]_3SiCl_3$. A solution of $C[Si(CH_3)_3]_3SiCl_3$[23] (2.30 g, 6.28 mmol) in 5.13 M ICl in CCl_4 (30 ml, 153.9 mmol) was stirred under N_2 for 6 hours at room temperature. The excess ICl was destroyed by cautiously shaking the mixture with saturated aqueous sodium thiosulfate (50 ml). The organic layer was separated, washed with water, separated, dried over $MgSO_4$ and the solvent removed under vacuum to leave a pale yellow solid. The desired product was extracted into chloroform. Removal of the chloroform left shiny yellow crystals which were sublimed under vacuum (0.2 mmHg, 150–180 °C) to give white crystals identified as *tris(chlorodimethylsilyl)trichlorosilylmethane*, $C[Si(CH_3)_2Cl]_3SiCl_3$ (2.4 g, 83% yield). Mp >320 °C. ^{1}H NMR: δ 0.91 [s, $Si(CH_3)_2$]. Proton coupled ^{29}Si: δ 0.18 (s, $SiCl_3$), 22.64 (m, $Si(CH_3)_2Cl$, $^2J_{Si-H}$ = 6.7 Hz); *m/z* (based on ^{35}Cl) 411 (100%, $[M - CH_3]^+$), 391 (5%, $[M - Cl]^+$), 303 (30%), 283 (45%), 93 (45%, $[Si(CH_3)_2Cl]^+$). Accurate *m/z* for $[M - CH_3]^+$ 410.8349 (calc. 410.8352), actual isotope pattern for $[M - CH_3]^+$ matches computer simulation.

Reaction of $C[Si(CH_3)_3]_3SiCl_3$ with IBr. The chlorosilane, $C[Si(CH_3)_3]_3SiCl_3$ (0.81 g, 2.22 mmol), was added to a 7.45 M solution of IBr in CCl_4 (10 ml, 74.5 mmol). The mixture was left stirring under N_2 for 6 hours after which the ^{1}H NMR spectrum was consistent with the presence of a mixture of $C[Si(CH_3)_3]_3SiCl_3$, $C[Si(CH_3)_2Br][Si(CH_3)_3]_2SiCl_3$ and CH_3I; $C[Si(CH_3)_3]_3SiCl_3$ (80%): δ 0.38 $[Si(CH_3)_3]$; $C[Si(CH_3)_2Br][Si(CH_3)_3]_2SiCl_3$ (20%): δ 0.48 $[Si(CH_3)_3]$, 0.96 $[Si(CH_3)_2Br)]$; CH_3I: δ 2.66 (CH_3). The mixture was left stirring at room temperature for a further five days after which the ^{1}H NMR spec-

trum indicated the presence of a trace amount of $C[Si(CH_3)_3]_3SiCl_3$ and a 2:1 mixture of $C[Si(CH_3)_2Br][Si(CH_3)_3]_2SiCl_3$ and $C[Si(CH_3)_2Br]_2[Si(CH_3)_3]SiCl_3$; $C[Si(CH_3)_2Br]_2[Si(CH_3)_3]SiCl_3$: δ 0.57 [$Si(CH_3)_3$], 1.05 [$Si(CH_3)_2Br$)]. After 28 days the ^{1}H NMR spectrum had changed little from the one observed after 5 days, and so the reaction was not followed up further.

Reduction of $C[Si(CH_3)_2Cl]_3SiCl_3$ with $LiAlH_4$. A mixture of $C[Si(CH_3)_2Cl]_3SiCl_3$ (0.98 g, 2.29 mmol) and $LiAlH_4$ (0.50 g, 13.17 mmol) in dry THF under N_2 was boiled under reflux for 6 hours. The excess $LiAlH_4$ was destroyed by carefully adding the mixture to 10% aqueous tartaric acid (100 ml) and the product extracted with hexane. Following separation, the solvent was removed under reduced pressure to give an oily liquid which was found by ^{1}H NMR spectroscopy to be a mixture of $C[Si(CH_3)_2H]_3SiH_3$, $C[Si(CH_3)_2H]_3H$,[24] and other unidentified compounds. Reducing the reflux time to 2 hours with the same amount of $LiAlH_4$ gave the same results as above so the reduction was carried out with half the amount of $LiAlH_4$ at room temperature. After 24 hours, the ^{1}H NMR spectrum of a sample of the reaction mixture showed the presence of the starting material, $C[Si(CH_3)_2H]_3SiH_3$ and a small amount of $C[Si(CH_3)_2H]_3H$. After a further 24 hours of stirring only $C[Si(CH_3)_2H]_3H$ could be identified by ^{1}H NMR spectroscopy.

Preparation of $C[Si(CH_3)_2H]_3SiH_3$. A mixture of $LiAlH_4$ (1.88 g, 49.5 mmol), benzyltriethylammonium chloride (0.38 g, 1.67 mmol), $C[Si(CH_3)_2Cl]_3SiCl_3$ (1.782 g, 4.17 mmol) and dry toluene (40 ml) was boiled under reflux under a dry N_2 atmosphere for 6 h. The mixture was left to cool and then filtered through a sintered glass funnel to leave the inorganic salts. A vacuum of 2 mmHg was applied to the solution and the desired product collected as white shiny crystals in a liquid nitrogen cooled trap. The crystals were identified as *tris(dimethylsilyl)silylmethane*, $C[Si(CH_3)_2H]_3SiH_3$, (0.37 g, 40% yield). Mp 67 °C. ^{1}H NMR: δ 0.22 [d, 18H, $Si(CH_3)_2H$, $^3J_{Me-H}$ = 3.96 Hz], 3.64 (s, 3H, SiH_3), 4.07 [sept, 3H, $Si(CH_3)_2H$]. Proton coupled ^{29}Si NMR: δ 13.77 (d of m, $Si(CH_3)_2H$, $^1J_{Si-H}$ = 188 Hz), −61.28 (qq, SiH_3, $^1J_{Si-H}$ = 200 Hz, $^3J_{Si-H}$ = 3.5 Hz); *m/z*: 219 (5%, $[M - H]^+$), 205 (25, $[M - CH_3]^+$), 173 (10), 115 (20), 113 (25), 95 (30), 93 (95), 73 (55, $[Si(CH_3)_3]^+$), 65 (45), 63 (40), 59 (30, $[Si(CH_3)_2H]^+$). Accurate mass for $[M - H]^+$ 219.086 (calc. 219.088). IR (Nujol): 2140.3 cm^{-1} (s, SiH_3), 2110.0 (s, $Si(CH_3)_2H$).

Preparation of $C[Si(CH_3)_2OH]_3Si(OH)_3$. In a 100 ml two necked round bottom flask cooled to −10–0 °C with the aid of an ice/salt bath, the silane $C[Si(CH_3)_2H]_3SiH_3$ (0.06 g, 0.27 mmol) was stirred with a dimethyldioxirane solution (0.038 M, 50 ml)[25] under N_2 for 8 hours. The solvent was removed under vacuum to leave a white solid identified as *trihydroxysilyltris[(hydroxy)dimethylsilyl]methane*, $C[Si(CH_3)_2OH]_3Si(OH)_3$, (0.081 g, 95% yield). Mp 85 °C (decomp.). ^{1}H NMR (acetone-d_6): δ 0.51 [s, $Si(CH_3)_2OH$]; the OH signal could not be assigned. Proton coupled ^{29}Si NMR (acetone-d_6): δ 10.47 [m, $Si(CH_3)_2OH$, $^2J_{Si-H}$ = 6.7 Hz], −42.53 [s, $Si(OH)_3$]; *m/z* 283 (20%, $[M–H_2O–CH_3]^+$), 265 (100, $[M–2H_2O–CH_3]^+$), 249 (95), 205 (40), 125 (40). Accurate mass for $[M–H_2O–CH_3]^+$ 283.033 (calc. 283.031). IR (KBr disc): 3350 cm^{-1} (b, H-bonded SiO–H).

Bromination of $C[Si(CH_3)_2H]_3SiH_3$. A 1 M solution of Br_2 in benzene was added dropwise to the silane (0.024 g, 0.1 mmol) under an atmosphere of dry N_2 and the reaction was monitored by ^{1}H NMR spectroscopy until all the Si–H had disappeared. The solvent was removed under vacuum to leave white shiny crystals identified as *tris(bromodimethylsilyl)tribromosilylmethane*, $C[Si(CH_3)_2Br]_3SiBr_3$ (0.075 g, 100% yield). Mp >320 °C. ^{1}H NMR (at 25 °C): δ 1.2 [broad s, $(CH_3)_2SiBr$.] ^{29}Si NMR (at 50 °C): δ 18.66 [s, $(CH_3)_2SiBr$], −36.59 (s, $SiBr_3$); *m/z* (based on ^{79}Br) 679 (30%, $[M - CH_3]^+$), 615 (100, $[M - Br]^+$), 527 (20), 461 (60), 397 (17), 137 (25, $[Si(CH_3)_2Br]^+$), 73 (35, $[Si(CH_3)_3]^+$). Accurate mass for $[M - CH_3]^+$ 678.525 (calc. 678.529). Computer simulation of $[M - CH_3]^+$ ion matches the acquired spectrum.

Partial bromination of $C[Si(CH_3)_2H]_3SiH_3$. The silane (0.185 g, 0.84 mmol) was dissolved in benzene (2 ml) and a bromine solution (0.63 M, 2.0 ml in benzene) was added dropwise while the silane solution was being stirred. After an hour of further stirring at room temperature, the ^{1}H NMR spectrum of a sample showed a mixture of $C[Si(CH_3)_2Br][Si(CH_3)_2H]_2SiH_3$, $C[Si(CH_3)_2Br]_2[Si(CH_3)_2H]SiH_3$, $C[Si(CH_3)_2Br]_3SiH_3$ and a trace amount of the starting material to be present. ^{1}H NMR (33%): $C[Si(CH_3)_2Br][Si(CH_3)_2H]_2SiH_3$: δ 0.31 [d, $Si(CH_3)_2H$, $^2J_{Me-H}$ = 3.96 Hz], 0.69 [s, $Si(CH_3)_2Br$], 3.69 (s, SiH), 4.0–4.2 [m, $Si(CH_3)_2H$]; $C[Si(CH_3)_2Br]_2[Si(CH_3)_2H]SiH_3$ (33%): δ 0.41 [d, $Si(CH_3)_2H$, $^2J_{Me-H}$ = 3.63 Hz], 0.79 [s, $Si(CH_3)_2Br$], 3.75 (s, SiH), 4.0–4.2 [m, $Si(CH_3)_2H$]; $C[Si(CH_3)_2Br]_3SiH_3$ (33%): δ 0.90 [s, $Si(CH_3)_2Br$], 3.82 (s, SiH). The Si–H signals for the $Si(CH_3)_2H$ groups overlap (4.0–4.2 ppm) and cannot be distinguished. More of the bromine solution (0.28 mmol) was added and the solution was left stirring overnight. A ^{1}H NMR spectrum of a sample of the products after that was consistent with the presence of a mixture of $C[Si(CH_3)_2Br]_3SiH_3$, $C[Si(CH_3)_2Br]_3SiBrH_2$, and $C[Si(CH_3)_2Br]_3SiBr_2H$. ^{1}H NMR: $C[Si(CH_3)_2Br]_3SiH_3$ as above; $C[Si(CH_3)_2Br]_3SiBrH_2$, (50%): δ 1.00 [s, $Si(CH_3)_2Br$], 4.82 (s, SiH); $C[Si(CH_3)_2Br]_3SiBr_2H$, (10%): δ 1.10 [s, $Si(CH_3)_2Br$], 5.65 (s, SiH).

Ab initio calculations

Calculations were performed on a DEC Alpha APX 1000A workstation using the GAUSSIAN94 program,[26] with the larger calculations run on a DEC 8400 superscalar cluster equipped with 10 fast processors, 6 GB of memory and 150 GB disk (resource of the UK Computational Chemistry Facility).

Geometry optimisations. An extensive search of the potential energy surface was undertaken at the 3–21G*[27–29]/HF level in order to locate all structurally stable conformers. In total eleven minima were found, corresponding to three structures with C_3 symmetry and eight with C_1 (see Fig. 2). Further geometry optimisations were then undertaken for all minima with the 6-31G* basis set[30–32] at the HF and MP2 levels of theory.

Frequency calculations. Vibrational frequencies were calculated from analytic second derivatives at the 3–21G*/HF and 6-31G*/HF levels to confirm all conformers as local minima on the potential energy surface. The force constants obtained from the 6-31G*/HF calculations were subsequently used to construct harmonic force fields using the ASYM40 program.[33] As no fully assigned vibrational spectra are available for this compound to scale the force fields, scaling factors of 0.9, 0.85 and 0.8 were adopted for bond stretches, angle bends and torsions, respectively, with values chosen falling within acceptable guidelines as suggested by Rauhut and Pulay.[34] The scaled harmonic force fields were then used to provide estimates of amplitudes of vibration (u) for use in the GED refinements.

Potential energy surface scan. To establish the eleven minima found on the potential energy surface as distinct features with appreciable barriers to internal rotation, a rigid scan of the potential energy surface connecting the minima corresponding to conformers 'cca' and 'ccb' was undertaken at the 6-31G*/HF level. The geometry of the molecule was frozen with the exception of the one dihedral angle required to convert from conformer 'cca' to 'ccb', which was stepped in twelve increments of 10.2°. Single-point energy calculations were then performed for each new value of the dihedral angle.

Table 7 GED data analysis parameters for $C[Si(CH_3)_2H]_3SiH_3$

Camera distance/mm	Weighting functions/Å^{-1}					Correlation parameter	Scale factor, k [a]	Electron wavelength[b]/Å
	Δs	s_{min}	sw_1	sw_2	s_{max}			
247.59	0.2	2.0	4.0	10.0	11.0	0.3350	0.930(6)	0.06016
95.63	0.4	8.0	10.0	30.4	35.6	0.4011	0.919(20)	0.06016

[a] Figures in parentheses are the estimated standard deviations. [b] Determined by reference to the scattering patterns of benzene vapour.

Gas-phase electron diffraction (GED)

Electron scattering intensities were recorded on Kodak Electron Image photographic plates using the Edinburgh gas-phase electron diffraction apparatus,[35] operating at *ca.* 40 kV. Five plates (three from the long camera distance and two from the short distance) were recorded and converted into digital format using a computer-controlled PDS microdensitometer employing a 200 micron pixel size at the Royal Greenwich Observatory, Cambridge.[36] The sample and nozzle temperatures were maintained at *ca.* 373 K during the exposure periods. Standard programs were used for the data reduction with the scattering factors of Ross *et al*.[37] Nozzle-to-plate distances, weighting functions used to set up the off-diagonal weight matrix, correlation parameters, final scale factors and electron wavelengths for the measurements are collected in Table 7.

Acknowledgements

We thank the EPSRC for financial support of the Edinburgh Electron Diffraction Service (grant GR/K44411) and for the Edinburgh *ab initio* facilities (grant GR/K04194). We also thank the UK Computational Chemistry Facility (admin: Department of Chemistry, King's College London, Strand, London, UK WC2R 2LS) for the computing time on Columbus. P. C. M. wishes to thank the British Council for the award of a Commonwealth Scholarship.

References

1 See, for example, C. Eaborn, Y. Y. El-Kaddar and P. D. Lickiss, *Inorg. Chim. Acta*, 1992, **200**, 337.
2 See, for example, P. D. Lickiss, in *Comprehensive Organic Functional Group Transformations*, ed. A. R. Katritzky, O. Meth-Cohn and C. W. Rees, Pergamon, Oxford, 1995, vol. 6, p. 377.
3 See, for example J. R. Black, C. Eaborn, P. M. Garrity and D. A. R. Happer, *J. Chem. Soc., Perkin Trans. 2*, 1997, 1633; M. A. M. R. Al-Gurashi, G. A. Ayoko, C. Eaborn and P. D. Lickiss, *J. Organomet. Chem.*, 1995, **499**, 57; C. Eaborn, A. Kowalewska and W. A. Stanczyk, *J. Organomet. Chem.*, 1998, **560**, 41, and references therein.
4 R. Hager, O. Steigelmann, G. Muller, H. Schmidbaur, H. E. Robertson and D. W. H. Rankin, *Angew. Chem., Int. Ed. Engl.*, 1990, **29**, 201.
5 P. Kulpinski, P. D. Lickiss and W. Stanczyk, *Bull. Pol. Acad. Sci.*, 1992, **40**, 21.
6 C. Eaborn and P. D. Lickiss, *J. Organomet. Chem.*, 1985, **294**, 305.
7 S. S. Dua, C. Eaborn, D. A. R. Happer, S. P. Hopper, K. D. Safa and D. R. M. Walton, *J. Organomet. Chem.*, 1979, **178**, 75.
8 C. Eaborn, P. B. Hitchcock and P. D. Lickiss, *J. Organomet. Chem.*, 1983, **252**, 281.
9 S. M. Whittaker, PhD Thesis, University of Salford, 1993.
10 V. N. Gevorgyan, L. M. Ignatovich and E. Lukevics, *J. Organomet. Chem.*, 1985, **284**, C31.
11 P. C. Masangane, Imperial College, London, unpublished work.
12 N. M. K. El-Durini and R. A. Jackson, *J. Chem. Soc., Perkin Trans. 2*, 1993, 1275.
13 P. D. Lickiss, D.Phil. Thesis, University of Sussex, 1983.
14 C. Eaborn, P. B. Hitchcock, A. Pidcock and K. D. Safa, *J. Chem. Soc., Dalton Trans.*, 1984, 2015.
15 A. G. Avent, S. G. Bott, J. A. Ladd, P. D. Lickiss and A. Pidcock, *J. Organomet. Chem.*, 1992, **427**, 9.
16 W. Kemp, *NMR in Chemistry: A Multinuclear Introduction*, Macmillan Education Ltd., London, 1986.
17 M. McPartlin, University of North London, personal communication.
18 P. D. Lickiss, *Adv. Inorg. Chem.*, 1985, **42**, 147.
19 R. Damrauer and R. J. Linerman, *J. Organomet. Chem.*, 1982, **235**, 1.
20 S. S. Al-Juaid, N. N. Buttrus, R. I. Damja, Y. Derouiche, C. Eaborn, P. B. Hitchcock and P. D. Lickiss, *J. Organomet. Chem.*, 1989, **371**, 287.
21 S. S. Al-Juaid, C. Eaborn, P. B. Hitchcock and P. D. Lickiss, *J. Organomet. Chem.*, 1988, **353** 297.
22 A.J. Blake, P. T. Brain, H. McNab, J. Miller, C. A. Morrison, S. Parsons, D. W. H. Rankin, H. E. Robertson and B. A. Smart, *J. Phys. Chem.*, 1996, **100**, 12280; P. T. Brain, C. A. Morrison, S. Parsons and D. W. H. Rankin, *J. Chem. Soc., Dalton Trans.*, 1996, 4589.
23 Z. A. Aiube and C. Eaborn, *J. Organomet. Chem.*, 1984, **269**, 217; S. S. Dua, C. Eaborn, D. A. R. Happer, S. P. Hopper, K. D. Safa and D. R. M. Walton, *J. Organomet. Chem.*, 1979, **178**, 75.
24 C. Eaborn, P. B. Hitchcock and P. D. Lickiss, *J. Organomet. Chem.*, 1983, **252**, 281.
25 R. W. Murray and R. Jeyaraman, *J. Org. Chem.*, 1985, **50**, 2847.
26 Gaussian 94 (Revision C.2), M. J. Frisch, G. W. Trucks, H. B. Schlegel, P. M. W. Gill, B. G. Johnson, M. A. Robb, J. R. Cheesman, T. A. Keith, G. A. Petersson, J. A.Montgomery, K. Raghavachari, M. A. Al-Laham, V. G. Zakrzewski, J. V. Ortiz, J. B. Foresman, J. Cioslowski, B. B. Stefanov, A. Nanayakkara, M. Challacombe, C. Y. Peng, P. Y. Ayala, W. Chen, M. W. Wong, J. L. Andres, E. S. Replogle, R. Gomperts, R. L. Martin, D. J. Fox, J. S. Binkley, D. J. Defrees, J. Baker, J. P. Stewart, M. Head-Gordon, C. Gonzalez and J. A. Pople, Gaussian Inc., Pittsburgh, PA, 1995.
27 J. S. Binkley, J. A. Pople and W. J. Hehre, *J. Am. Chem. Soc.*, 1980, **102**, 939.
28 M. S. Gordon, J. S. Binkley, J. A. Pople, W. J. Pietro and W. J. Hehre, *J. Am. Chem. Soc.*, 1982, **104**, 2797.
29 W. J. Pietro, M. M. Francl, W. J. Hehre, D. J. Defrees, J. A. Pople and J. S. Binkley, *J. Am. Chem. Soc.*, 1982, **104**, 5039.
30 J. Hehre, R. Ditchfield and J. A. Pople, *J. Chem. Phys.*, 1972, **56**, 2257.
31 P. C. Hariharan and J. A. Pople, *Theor. Chim. Acta*, 1973, **28**, 213.
32 M. S. Gordon, *Chem. Phys. Lett.*, 1980, **76**, 163.
33 ASYM40 version 3.0, update of program ASYM20. L. Hedberg and I. M. Mills, *J. Mol. Spectrosc.*, 1993, **160**, 117.
34 G. Rauhut and P. Pulay, *J. Phys. Chem.*, 1995, **99**, 3093.
35 C. M. Huntley, G. S. Laurenson and D. W. H. Rankin, *J. Chem. Soc., Dalton Trans.*, 1980, 954.
36 J. R. Lewis, P. T. Brain and D. W. H. Rankin, *Spectrum*, 1997, **15**, 7.
37 A. W. Ross, M. Fink and R. Hilderbrandt, in *International Tables for Crystallography*, ed. A. J. C. Wilson, Kluwer Academic Publishers, Dordrecht, 1992, vol. C, p. 245.

Paper 9/02915J